https://doi.org/10.1016/j.mtcomm.2020.101144

A strong correlation between the bending rigidity and the length of single-walled carbon nanotubes

Haidong Liang[1], Qi Wang[2], Baoling Huang[2], Haimin Yao[3], Linghui He[1,4], Youdi Kuang[1*]

[1]School of Mechanics and Construction Engineering, MOE Key Laboratory of Disaster Forecast and Control in Engineering, Jinan University, Guangzhou, China

[2]Department of Mechanical and Aerospace Engineering, Hong Kong University of Science and Technology, Clear Water Bay, Kowloon, Hong Kong, China

[3]Department of Mechanical Engineering, Hong Kong Polytechnic University, Hung Hom, Kowloon, Hong Kong, China

[4]Depart of Modern mechanics, University of Science and Technology of China, Hefei, China

* Corresponding author: ykuang@jnu.edu.cn

Highlights

- The bending rigidity of single walled carbon nanotubes strongly correlates to the tube length due to the honeycomb lattice structure. The rigidity increases with the tube length and converges to the value predicted by classical continuum theories.
- The nonlocal parameter of single walled carbon nanotubes for nonlocal continuum modeling is almost independent of the chirality and linearly increases with the tube diameter with a scale factor 1.5.

Abstract

Continuous efforts to discover the novel carbon nanotube ultrahigh frequency resonators or sensors have being made since past two decades. The bending rigidity plays a key role in determining the frequency magnitude. Although it is previously justified that the bending rigidity has the almost linear dependence on the cubic of tube diameter, its dependence on another characteristic scale, i.e., the tube length is missing. Considering that the direct experimental observation faces significant

challenge due to the low measurement precision by the inevitable thermodynamic fluctuation, we theoretically explored such size effect by means of three approaches respectively at different scale levels including quantum mechanics lattice dynamics calculations, molecular mechanics simulations and nonlocal continuum modeling for single-walled carbon nanotubes. The results from the different approaches give the consistent conclusion that there exists a strong correlation between the tube length and the bending rigidity, i.e., the rigidity increases with the tube length and converges to the value predicted by continuum theories. Moreover, we also find the nonlocal parameter reflecting the microscopic lattice effect in present continuum modeling almost independent of the chirality and linearly increases with the tube diameter with a scale factor 1.5. The comprehensive study may not only guide the design of ultrahigh frequency carbon nanotube devices but also provide insight to the bending nanomechanics of other devices made from nanotubes, nanobeams and nanowires.

Keywords: Carbon nanotubes, bending rigidity, Lattice dynamics, Molecular mechanics, nonlocal continuum theories

1. Introduction

Different with bulk nanomaterials, single-walled carbon nanotubes (SWCNTs) [1] have quasi-one-dimensional hollow cylinder structure comprised of hexagonal carbon ring. The quasi-one-dimensional nature makes them possess a basic mechanical parameter, the bending rigidity. The bending rigidity determines their static buckling resistance under axial or bending loading [2,3], the thermodynamic stability of CNTs [4] in ambient environments, the vibrational frequencies of the CNT as high frequency resonators [5-8] and the sensitivity of the CNT as high frequency sensors [9] to detect small molecule. The mode frequency of a CNT resonator or sensor can be up to GHz magnitude; this means that a slight variation in the bending rigidity will give rise to significant change in magnitude of mode frequency. In other words, the performance of a CNT resonator or sensor greatly depends on the characterization precision of the bending rigidity. Therefore, the effective characterization of the bending rigidity is critically important. Based on classical continuum theories

Yakobson et al. [10] proposed a formula $D = \pi C R^3$ to characterize the intrinsic bending rigidity D in the long wavelength limit, $C = 342$ N/m, R the radius of SWCNTs. The effect of the honeycomb microstructure on the bending rigidity was neglected in the formula. The similar relation was also found by Guo and Zhang [11] using the molecular mechanics (MM) model and deformation mapping technique. Ru [12] argued that the bending rigidity of SWCNTs should be regarded as a material parameter independent of representative thickness in the continuum formula [13]. Actually, the thickness parameter indeed disappears in the formula by Yakobson et al. [10]. Previous molecular dynamics simulations [14] showed that the bending rigidity approximately satisfies the above formula while no results on the effect of sample length were reported by such an approach. On the experimental side [15], due to the challenge in measurements, the length effect on the bending rigidity was hard to observe. To investigate the length effect, some authors [16-20] tried to consider the nonlocal effect [21], i.e., the microstructure effect into classical continuum models and found that different nonlocal continuum theories gave even opposite conclusions. Moreover, the nonlocal parameter reflecting the microstructure effect is usually achieved from experiments or quantum mechanics calculations, but no such data were provided so far for SWCNTs. Therefore, we characterize the bending rigidity using quantum mechanics lattice dynamics (LD) calculations and MM simulations, respectively. Both results suggest that the bending rigidity increases with the sample length and gradually converges to the value predicted by $D = \pi C R^3$ in the long wavelength limit, indicating the strong correlation between the bending rigidity and the sample length. We also present the value of nonlocal parameter of SWCNTs by means of quantum mechanics LD results.

The paper is organized as follows: we firstly character the bending rigidity of SWCNTs by the approach of quantum mechanics LD. The effects of radius, chirality and length (equivalently the wavelength) of SWCNTs on the bending rigidity are explored. MM simulations are then conducted to characterize the bending rigidity of

SWCNTs. The corresponding results are discussed and compared with those by quantum mechanics LD calculations. We further extract the nonlocal parameters reflecting the microstructure effect by comparing the dispersion relations respectively by the appropriate nonlocal continuum theory and quantum mechanics LD calculations. The effects of radius and chirality on the nonlocal parameter are discussed. The conclusive remarks are given at the end.

2. The bending rigidity of SWCNTs by quantum mechanics lattice dynamics calculations

Based on LD theories [22]， the harmonic interaction force constant (HIFCs) of SWCNTs are calculated using the self-consistent charge density functional tight-binding approach [23]. We note that this approach well reproduces the experimental phonon dispersion of graphite [24]. Before calculating HIFCs the corresponding lattices are fully optimized with a convergence precision of 1×10^{-8} eV/Å for the atomic force. As calculating HIFCs, a convergence standard of 1×10^{-9} is used for the self consistence of charge density. The vacuum layer thickness in each SWCNT sample is taken 1.5 nm as least. The constrains including the translational symmetries, the point group symmetries and the rotational invariance conditions are applied to HIFCs via a least-squares method [25]. The phonon dispersion relation between frequency ω and wavevector $\mathbf{q}$ of each SWCNT is then achieved by the open source code Phonopy [26] after inputs of HIFCs. In the long wavelength limit $q\to0$, the dispersion of flexural acoustic (FA) modes [27] should satisfy $\omega^2=\frac{D}{m_p}q^4$, m_p the mass of unit length of SWCNT. This means that we may extract the bending rigidity D from the quadratic dispersion data using $D=\underset{\omega,q\to0}{\omega^2 m_p/q^4}$.

We calculate the phonon dispersions for armchair and zigzag SWCNTs with radius R ranged from 0.2 nm to 0.69 nm. Representatively, the full dispersions of the (8,8)

SWCNT are plotted in Fig.1. This tube has four acoustic branches among which the lowermost two are degenerated and correspond to the FA modes. The other two correspond to the torsional acoustic (TA) and longitudinal acoustic (LA) modes. The

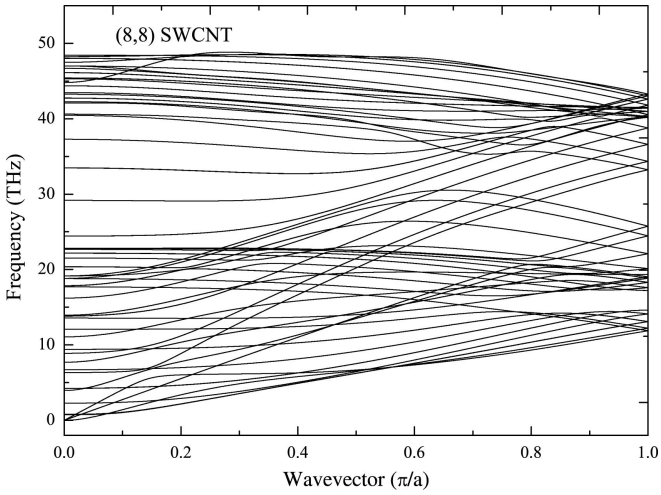

Fig.1 The full phonon dispersions of the (8, 8) SWCNT by our quantum mechanics LD calculations.

LA modes usually have higher frequency than that of TA modes as the axial Young's modulus is larger than the shear modulus. Using the low frequency data corresponding to very small q, i.e., $q \le \frac{\pi}{1000a}$, a the equilibrium lattice constant of the tube, we calculate D of all tubes considered. As shown in Fig.2, the obtained D satisfies $D = \pi C R^3$ with the constant C=338 N/m. The results well agree with those by Yakobson et al. [10]. In the long wavelength limit, the microstructure effect may be neglected due to the wavelength is far larger that the lattice constant. This is the reason for the consistence of results by completely different two approaches, i.e., the LD calculations and the continuum model [10]. For the moderate wavelengths the

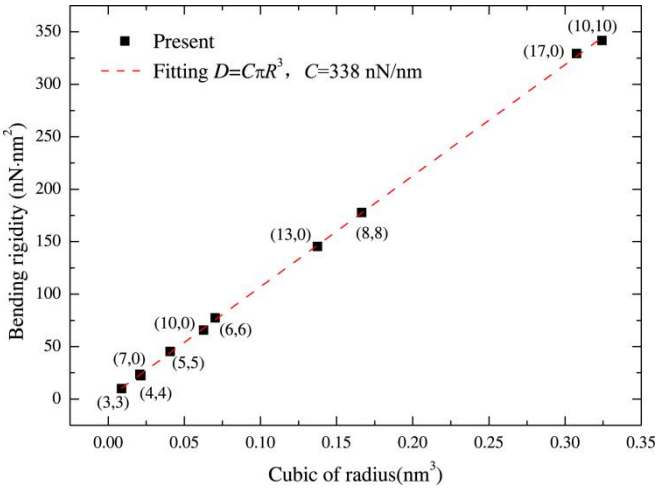

Fig.2. The relation between the bending rigidity and the radius of SWCNTs in the long wavelength limit.

microstructure effect will plays a role. To demonstrate this, we define the effective bending rigidity D_e at different wavelength λ. Here $\lambda = \frac{2\pi}{q}$, $D_e = \frac{\lambda^4 \omega^2 m_p}{16\pi^4}$. Obviously, $D_e = D$ only in the long wavelength limit. We plot the relation $\lambda \sim D_e$ of the (8, 8) SWCNT in Fig.3. It can be seen that D_e drastically increases as

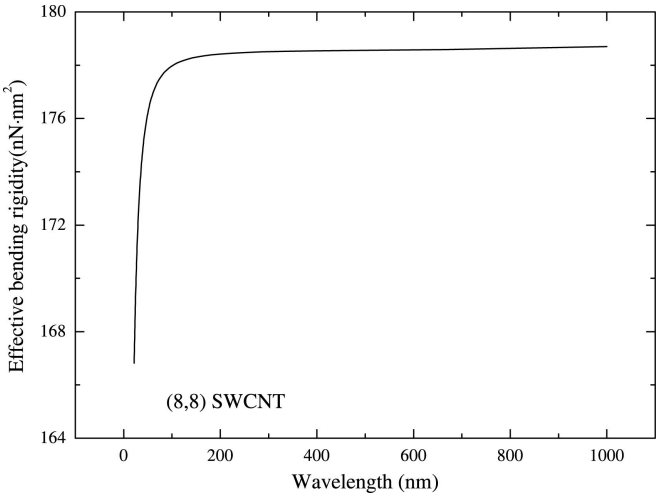

Fig.3. The dependence of the effective bending rigidity of the (8, 8) SWCNT on the wavelength.

$\lambda < 200$ nm and nearly converges to D at λ=400 nm. This trend is also observed in

other SWCNTs, indicating that the bending rigidity of the SWCNT strongly correlates to its length due to the honeycomb lattice structure. In classical continuum theories it is assumed that the material is continuous in space. Consequently, the bending rigidity of a rod like structure is independent on its length.

3. The bending rigidity of SWCNTs by molecular mechanics simulations

We have calculated the bending rigidity of SWCNTs by the quantum mechanics LD approach which bases on the reciprocal space. To further our understanding on the length dependence, we would like to conduct real space MM simulations. The optimized Tersoff empirical potential [28] which well reproduced the phonon dispersion of SWCNTs is used to describe the atomic interactions in SWCNTs. The simulation procedures are as follows: for a SWCNT with the given length, the atoms at its left end are fixed and the left part is free. This corresponds to the clamped-free mechanical boundary condition. After a series of forces F_i (i=1,2,3,4) vertical to the axis are applied to the atoms at the right end, the corresponding displacement responses d_i are recorded. Before loading, the initial sample is fully optimized and relaxed to a zero-stress state. After obtaining the numerical $F_i \sim d_i$ relation, we may estimate the effective bending rigidity D_e using the formula $D_e = \frac{F_i L^3}{3d_i}$ from the elementary beam theory [29]. The same procedures are then taken for SWCNTs with different sample length to observe how D_e changes with the length. We also consider the clamped-clamped mechanical boundary condition, i.e., the atoms at each end are fixed. The loading F_i is applied at the middle of the tube for the boundary condition. Correspondingly, the effective bending rigidity D_e is estimated by the formula [29] $D_e = \frac{F_i L^3}{192 d_i}$. All simulations are done using the open source code

Lammps [30] distributed by Sandia National Laboratories.

As indicated by the corresponding formulas, the numerical relation $F_i \sim d_i$ from simulations should be linear in order to precisely estimate D_e. Representatively, the displacement responses of the (5, 5) SWCNT having a length 14.8 nm under different boundary conditions are shown in Fig.4a and Fig.4b. The observed linear responses

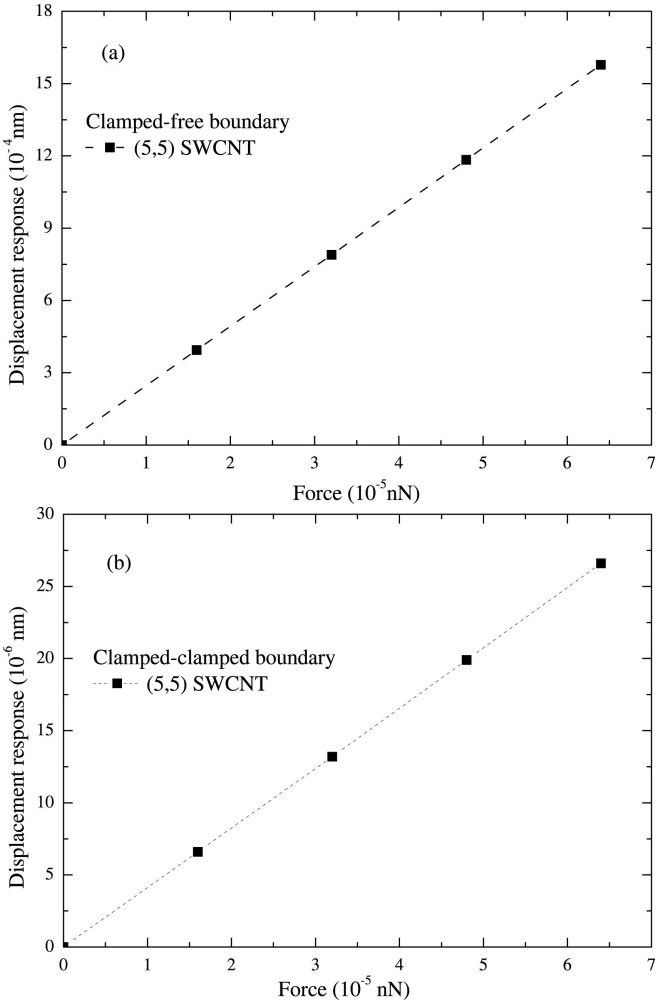

Fig.4. Plots of the linear relation between the force and the displacement response of the (5,5) SWCNT respectively under (a) clamped-free and (b) clamped-clamped boundary conditions.

indicate that our results are reliable. Fig.5a shows the dependence of D_e on the slender ratio of the (5, 5) and (10, 0) SWCNTs under the clamped-free boundary condition. The slender ratio is defined as the ratio of the sample length to the tube

diameter. We can see that D_e increases with the slender ratio and gradually converges to D. The trend is consistent with that in Fig.3 by quantum mechanics LD calculations. We note that the shearing effect on D_e in our MM simulations is less than 0.5% as the slender ratio is larger than 15. The total increase magnitude defined by $(D - D_e)/D_e$ is up to 5% at least, showing that the shearing effect is not the

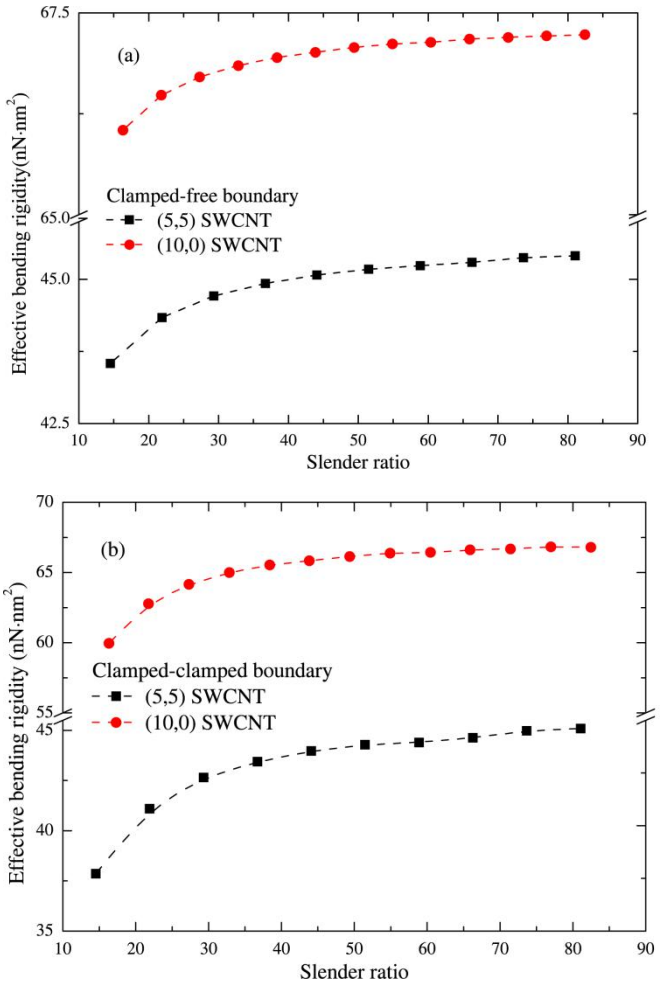

Fig.5. Plots of the dependence of effective bending rigidity on the slender ratio for (5, 5) and (10, 0) SWCNTs respectively under (a) clamped-free and (b) clamped-clamped boundary conditions.

reason for the trend. For the clamped-clamped boundary condition the same trend is also observed for the (5, 5) and (10,0) SWCNTs, as shown in Fig.5b. The slender ratio used in our MM simulations is less than 100 which is far smaller than the equivalent one (~1000) in Fi.g3. That is why the increase trend in Fig.3 looks sharp.

4. The nonlocal parameter of SWCNTs for nonlocal continuum modeling

LD calculations and MM simulations are the atom-based numerical approach. The corresponding computational costs are high especially for large SWCNTs. In contrast, continuum modeling with much higher computation efficiency has shown the ability in describing some mechanical behaviors of large SWCNTs without loss of basic physics. For example, it was argued [31] that the mechanical buckling of CNTs may be understood based on the corresponding continuous theories. Therefore, a question is that if we may describe the dependence of the bending rigidity on the sample length at the continuum level. In classical continuum theories the stress σ or strain ε is local, i.e., the stress is only related to the strain at a given material point, resulting in the failure of classical continuum theories in describing the microstructure effect. To consider the effect, the nonlocal continuum theories were developed and applied to dynamics of SWCNTs in literature [16,32,33]. As modeling the SWCNT as a beam, the one dimensional nonlocal constitutive relation [21] may be written as $\sigma-(e_0b)^2\frac{\partial^2\sigma}{\partial x^2}=E\varepsilon$, E the Young's modulus; b is an internal characteristic length and usually given as the bond length or the lattice constant in previous work [16,19,32,33]; e_0 is an adjustable parameter to match the corresponding results with those by experiments or quantum mechanics calculations. Based on the nonlocal constitutive relation and the Euler beam theories, the dispersion relation of SWCNTs may be deduced as [16] $\omega^2=\frac{D_e}{m_p[1+(e_0b)^2q^2]}q^4$. As $q\to 0$, q^2 is the negligible high order component of q in the term $1+(e_0b)^2q^2$, the formula will reduce to the classical form $\omega^2=\frac{D}{m_p}q^4$ in the long wavelength limit $q\to 0$. We note that in the formula $\omega^2=\frac{D_e}{m_p[1+(e_0b)^2q^2]}q^4$ the shearing effect is neglected considering the fact that this effect plays minor role for large sample length, as justified by our MM

simulations. For the moderate wavelength, we have $\frac{D_e}{D}=\frac{1}{1+4\pi^2(e_0b)^2/\lambda^2}$. This formula shows that the effective bending rigidity D_e increases with the wavelength λ, consistent with the conclusion by our LD calculations. By comparing the dispersion relations by the formula and our LD calculations, we extract the parameter e_0b defined as the nonlocal parameter for each SWCNT considered. The corresponding results are shown in Fig.6. It can be seen that e_0b is almost independent of chirality and linearly increases with the diameter with a scale factor 1.5. In known nonlocal continuum modeling e_0b was usually regarded as a constant for different SWCNTs. Therefore, present results shed substantial light on nonlocal continuum modeling of the tube like nanostructures. Taking $e_0b=1.5\times(2R)$, the effective bending rigidity of SWCNTs can also be correlated to their slender ratio

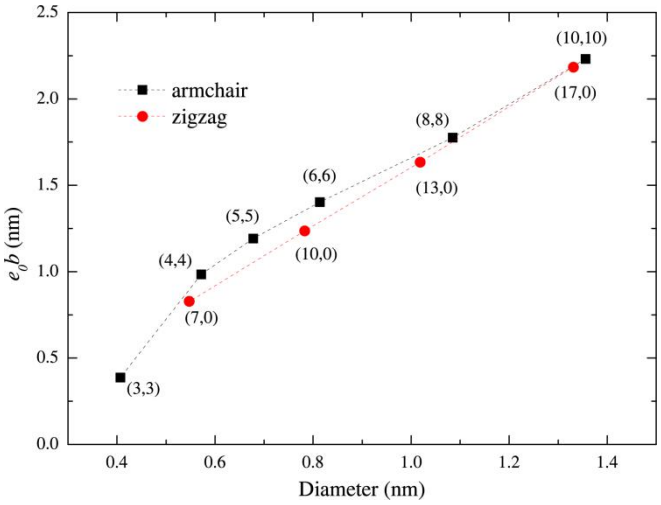

Fig.6. The dependence of the nonlocal parameter e_0b on the tube diameter.

defined by s as $D_e=\frac{\pi CR^3}{1+9\pi^2/s^2}$. The new formula shows that $D_e\to D$ as $s\to\infty$. Actually, it may help provide us with a reference of frequency error due to the neglection of length effect on the vibrational frequency of SWCNT sensors or resonators. To demonstrate this, taking a cantilever SWCNT with R=0.5 nm,

m_p=2.59×10^{-15} kg/m and s=20, its first order mode frequency ω_1 is calculated to be $\omega_1 = 1.875^2\sqrt{D_e/(16s^4R^4m_p)} = 56.92$ GHz, about 10% lower than that (~62.92 GHz) without considering the length effect. We note that although there exist several nonlocal continuum models [17], the present one [16] can give the analytic and comparable dispersion with ours. The development of advanced nonlocal continuum model is beyond the scope of this work.

5. Conclusive remarks

We have done a comprehensive study on the effect of SWCNT length on its bending rigidity using different approaches including quantum mechanics LD calculations, MM simulations and nonlocal continuum modeling. Both results from LD calculations and MM simulations show that the bending rigidity increases with the length and gradually converges, solving the argument on the length effect in previous nonlocal continuum modeling. By comparing the dispersions of SWCNTs respectively from LD calculations and the appropriate nonlocal continuum model, we find that the nonlocal parameter is independent on the tube chirality while linearly increases with the diameter. The present work may not only provide insight in understanding bending nanomechanics of SWCNTs but also serve as a benchmark study for other one-dimensional nanostructures such as nanobeams and nanowires.

Acknowledgements

B. H and H.Y are thankful for the financial support respectively from the Hong Kong General Research Fund under Grant No. 613413 and the National Natural Science Foundation of China under Grant No. 11772283. The data supporting the present conclusions are available once they are requested.

References

[1] S. Iijima, Nature 354 (1991) 56-58.

[2] O. Lourie, D.M. Cox, H. D.Wagner, Phys. Rev. Lett. 81 (1998) 1638.

[3] J.-P. Salvetat, J.-M. Bonard, N. Thomson, A. Kulik, L. Forro, W. Benoit, L. Zuppiroli,

Appl.Phys. A 69 (1999) 255-260.
[4] R. Duggal, M. Pasquali, Phys. Rev. Lett. 96 (2006) 246104.
[5] D. Garcia-Sanchez, A. San Paulo, M.J. Esplandiu, F. Perez-Murano, L. Forró, A. Aguasca, A. Bachtold, Phys. Rev. Lett. 99 (2007) 085501.
[6] I. Khivrich, A.A. Clerk, S. Ilani, Nat. Nanotechnol. 14 (2019) 161-167.
[7] A. Tavernarakis, A. Stavrinadis, A. Nowak, I. Tsioutsios, A. Bachtold, P. Verlot, Nat. commun. 9 (2018) 662.
[8] Y. Tsaturyan, A. Barg, E.S. Polzik, A. Schliesser, Nat. Nanotechnol. 12 (2017) 776-783.
[9] K. Jensen, K. Kim, A. Zettl, Nat. Nanotechnol. 3 (2008) 533-537.
[10] B.I. Yakobson, P. Avouris, Carbon nanotubes, Springer, 2001, p. 287-327.
[11] X. Guo, T. Zhang, J. Mech. Phys. Solids 58 (2010) 428-443.
[12] C. Ru, Phys. Rev. B 62 (2000) 9973.
[13] Y. Huang, J. Wu, K.-C. Hwang, Phys. Rev. B 74 (2006) 245413.
[14] D. Srivastava, C. Wei, K. Cho, Appl. Mech. Rev. 56 (2003) 215-230.
[15] R.S. Ruoff, D. Qian, W.K. Liu, Comptes Rendus Physique 4 (2003) 993-1108.
[16] P. Lu, H. Lee, C. Lu, P. Zhang, Int. J. Solids Stru 44 (2007) 5289-5300.
[17] J. Fernández-Sáez, R. Zaera, J. Loya, J. Reddy, Int. J. Eng. Sci. 99 (2016) 107-116.
[18] Q. Wang, V. Varadan, Smart Mater. Struct. 15 (2006) 659-666.
[19] C.W. Lim, Appl. Math. Mech. 31 (2010) 37-54.
[20] N. Challamel, C. Wang, Nanotechnology 19 (2008) 345703.
[21] A.C. Eringen, Nonlocal continuum field theories, Springer Science & Business Media, 2002.
[22] M. Born, K. Huang, Dynamical theory of crystal lattices, Clarendon press, 1954.
[23] M. Elstner, Theor. Chem. Acc 116 (2006) 316-325.
[24] Y. Kuang, L. Lindsay, B. Huang, Nano Lett. 15 (2015) 6121-7127.
[25] X. Wang, M. Kaviany, B. Huang, Nanoscale 9 (2017) 18022-18031.
[26] A. Togo, Avaliable: http://phonopy. sourceforge. net (2009).
[27] J. Carrete, W. Li, L. Lindsay, D.A. Broido, L.J. Gallego, N. Mingo, Mater. Res. Lett. 4 (2016) 204-211.
[28] L. Lindsay, D. A.Broido, Phys. Rev. B 81 (2010) 205441.
[29] J.R. Vinson, New York, Wiley-Interscience, 1974. 186 p (1974).
[30] S. Plimpton, P. Crozier, A. Thompson, Sandia National Laboratories 18 (2007) 43.
[31] B.I. Yakobson, C. J.Brabec, J. Bernholc, Phys. Rev. Lett. 76 (1996) 2511.
[32] K.M. Liew, Y. Hu, X. He, J. Comput. Theor. Nanos. 5 (2008) 581-586.
[33] L. Wang, H. Hu, Phys. Rev. B 71 (2005) 195412.